Surgical Endoscopy (2019) 33:620–632
https://doi.org/10.1007/s00464-018-6402-y

DYNAMIC MANUSCRIPT

# Fluorescence lymphangiography-guided full-thickness oncologic gastric resection

**Seong-Ho Kong[1,2] · Francesco Marchegiani[1] · Renato Soares[1] · Yu-yin Liu[3,4] · Yun-Suhk Suh[2] · Hyuk-Joon Lee[2,5] · Bernard Dallemagne[3] · Han-Kwang Yang[2,5] · Jacques Marescaux[1,3] · Michele Diana[1,3]**

Received: 15 January 2018 / Accepted: 20 August 2018 / Published online: 27 August 2018


## Abstract

**Background** We aimed to assess the feasibility of a novel hybrid endoscopic/laparoscopic non-exposed, full-thickness, single-wall gastric resection technique guided by a fluorescence lymphangiography to identify the lymphatic pathway and the sentinel node basin.

**Methods** Eight large white pigs (4 acute and 4 survival models) were included. Indocyanine green was injected submucosally around a pseudo-tumor at four points (1 ml, 0.1 mg/ml). The lymphatic spreading pathway was identified by the means of near-infrared (NIR) laparoscopic camera, and the resection line was planned outside of the fluorescent signals, to include all the potential lymphatic channels. Lymph node (LN) dissection was performed at greater curvature side and the infrapyloric area preserving the infragastric artery for all pigs. At the lesser curvature, 3–4 branches of the gastric artery were preserved in all acute and in two survival (group A), while in the remaining animals, 1–2 branches were preserved (group B). Perfusion of the remaining stomach was examined by NIR angiography. The gastric motility and function were evaluated by the means of a dynamic MRI immediately after the procedure and repeated after 1 week in surviving animals.

**Results** The hybrid full-thickness resection with bilateral sentinel LN basin dissection were successfully performed with no intra-operative or post-operative complications. The removed specimen was including all the area with florescent signal. The remaining stomach demonstrated a good perfusion at the NIR angiography. The dynamic MRI revealed a preserved emptying function in the acute animals and in the group A, and a loss of function in the group B.

**Conclusions** Fluorescence-lymphangiography guided hybrid resection was feasible to remove a relatively large part of the stomach including the lymphatic spreading pathway and sentinel basin. The extent of dissection in the lesser curvature side can affect the post-operative function and further researches are warranted to optimize the concept.

**Keywords** Near-infrared fluorescence guided surgery · Full-thickness resection · Sentinel node navigation surgery · Image guided surgery · Dynamic MRI · Capillary lactate test

Radical wide resection of the primary tumor and the lymph nodes is the standard treatment in the surgical management of gastric cancer, due to unpredicted spread of the cancer cells [1]. This approach is being challenged by new concepts of individually tailored surgery. The optimization of sentinel node navigation techniques, providing spatial information of cancer diffusion pathway, could enable a limited resection

This work was presented at the 25th EAES meeting, 14–17 June 2017, Frankfurt, Germany.

**Electronic supplementary material** The online version of this article (https://doi.org/10.1007/s00464-018-6402-y) contains supplementary material, which is available to authorized users.

✉ Michele Diana
michele.diana@ircad.fr; michele.diana@ihu-strasbourg.eu

[1] IHU Strasbourg, Institute of Image-Guided Surgery, Strasbourg, France

[2] Department of Surgery, Seoul National University Hospital, Seoul, South Korea

[3] IRCAD, Research Institute against Cancer of the Digestive System, 1, Place de l'Hôpital, 67091 Strasbourg, France

[4] Department of General Surgery, Chang Gung Memorial Hospital, Linkou, Chang Gung University, Taoyuan, Taiwan

[5] Cancer Research Institute, Seoul National University Hospital, Seoul, South Korea

of the lymph nodes in patient with negative lymph node metastasis, who comprises about 90% in stage I and 30% in stage II–III gastric cancer [2, 3].

Various limited tailored gastric resection techniques are under development [4]. Endoscopic submucosal resection has almost replaced surgery for treatment of early gastric cancer with almost no risk of lymph node metastasis (absolute indication) in Korea or Japan [5]. Although, there is an ongoing effort to apply the indications into a little bit deeper or wider cancer (expanded indication), the safety of expanded indication is still in doubt, especially for undifferentiated cancers [6]. Full-thickness resection (FTR) is suggested to provide better radicality when compared to an endoscopic submucosal dissection for cancer with possible lymph node metastasis, since there is a risk of residual cancer cells in the lymphatic structures in the deep gastric wall underneath the primary tumor site [7]. The assumption is that cancer emboli could be retained within the gastric wall outside the boundary of a round-shaped FTR, such as NEWS or CLEAN-NET techniques, which does not remove the lymphatic channels surrounding the primary tumor site (Fig. 1A) [4, 8].

Lymph node mapping, with peritumoral indocyanine green (ICG) injection and near-infrared fluorescent optic systems, has a better sensitivity to identify possible lymphatic metastasis pathway in the gastric wall, when compared to the use of vital dyes [9]. Therefore, the fluorescence-based lymphangiography could guide a patient-tailored resection which includes the primary tumor and the possible lymphatic metastasis pathway within the gastric wall.

Theoretically, a "fluorescent lymphangiography-guided tailored gastric wall resection" could improve radicality when compared to a standard "round-shaped" FTR and, if oncologically appropriate, could offer an organ-sparing alternative to radical surgical resection.

In cases in which the fluorescent lymphangiography highlights the lymphatic pathways as going to both the lesser and greater curvature, a wide local resection should be required to include all the possible lymphatics. However, such large resection involving the devascularization and/or the denervation of both lesser and greater curvature could result in functioning deterioration and/or ischemia in the remaining gastric wall [10].

The purpose of this experimental study was to assess the feasibility of a fluorescent lymphangiography-guided, single-wall segmental resection with dissection of bilateral (lesser and greater curvature) perigastric lymph nodes. Additionally, the impact of such extreme example of wide local resection on perfusion and motility function of the remaining gastric wall was assessed in the porcine model.

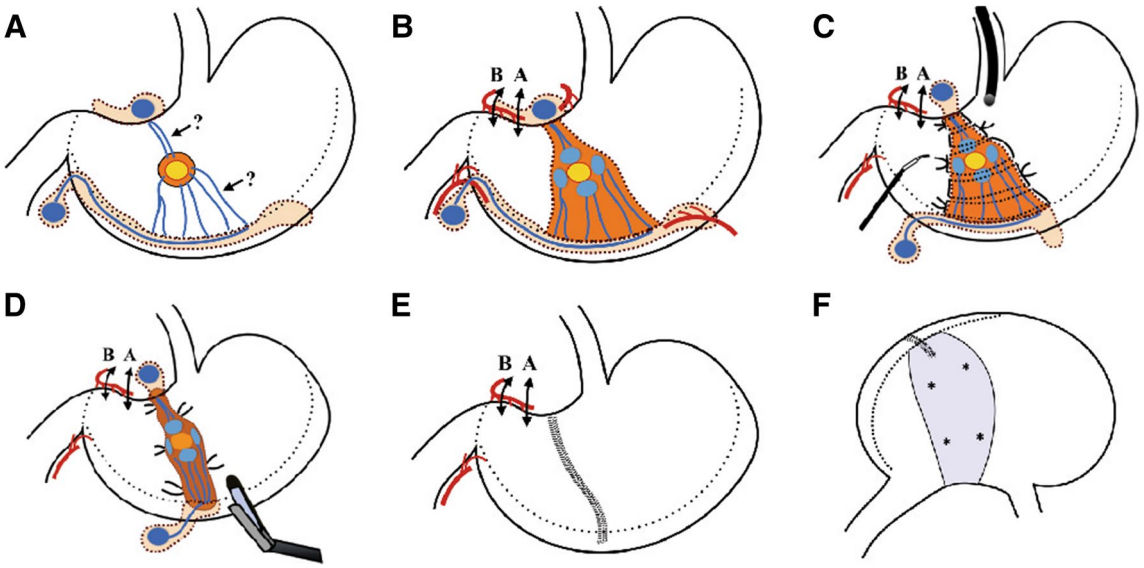


**Fig. 1** Scheme of fluorescent lymphangiography-guided single-wall segmental resection with bilateral lymph node basin dissection. **A** In case of round-shape full-thickness resection, there is a chance to leave the cancer cells in the intragastric lymphatic channels (question marks); **B** extent of the resection. Infrapyloric artery is preserved, and 3–4 or 1–2 branches of right gastric artery were preserved for group A and group B, respectively. **C–E** Hybrid resection of the stomach using a laparoscopic suture-passer and linear staplers. **F** Possible ischemic area in the posterior wall. * indicates the points for capillary lactate test

## Materials and methods

### Animals

A total of 8 Large White pigs (Sus scrofa domesticus; mean weight 32.5 ± 1.8 kg) were used. The animal experiment protocol received full approval by the local Ethical Committee on Animal Experimentation (ICOMETH) and by the French Ministry of Superior Education and Research (protocol number: 38.2015.01.077). All animals were managed according to the directives of the European Community Council (2010/63/EU). Pigs were fasted for 24 h before surgery with free access to water. Small amount of pine apple juice was given to pigs to stimulate the bowel movement 10 min before the premedication. Premedication by intramuscular injection of ketamine (20 mg/kg) and azaperone (2 mg/kg) (Stresnil; Janssen Cilag, Belgium) was administered 10 min before surgery. Induction was achieved by intravenous propofol (3 mg/kg), followed by totally intravenous anesthesia maintained with 0.17–0.2 mg/kg/min of propofol. No neuromuscular blocking agents were administered.

Four pigs were used for acute experiments to test the technical feasibility of the procedure, and were humanely sacrificed after the procedures, with an intravenous injection of a lethal dose of potassium chloride. The remaining four pigs survived for 7 days and were housed, after the first procedure, in individual cage, under controlled humidity and temperature conditions and provided with toys. A standardized diet was given (Porc Spot G S25; COSTAL, Molsheim, France), 700–750 g divided 2–3 times a day in the first 2 post-operative days (POD) and 1000–1050 g divided 2–3 times a day thereafter, until the midday of the 6th POD (total amounts: 5150–5250 g).

Activity and presence of adverse events were observed daily. The second evaluation was performed at POD7 under general anesthesia, as previously described. Body weight was recorded before the first procedure and at POD7. At the end of the second look procedure, animals were sacrificed with an intravenous injection of a lethal dose of potassium chloride under anesthesia.

### Operative procedures

A dynamic MRI was performed as described later, and the pig was placed in the supine position. Four or five 12 mm trocars were placed in the lower abdomen, and a pneumoperitoneum was established.

An imaginary tumor location (about 2–3 cm of diameter) was decided at the anterior wall of the body of the stomach. Normal saline (0.5 cc) was submucosally injected at the four corners of the pseudo-tumor to make blebs as a test injection to prevent extra-gastric leakage of ICG, and 0.5 cc of 0.2 mg/ml ICG was injected inside the saline bleb. Fluorescent signal indicating lymphatic channels in the gastric wall was observed by the laparoscopic near-infrared camera system (Karl Storz, Tuttlingen, Germany), and the resection line was planned and marked along the outmost lymphatic pathway using mono-polar cautery (Fig. 2).

LN dissection was performed in LN station 3, 4d, partial 4sb, and 6 (Figs. 1B, 2C–F). Left gastroepiploic artery was ligated after 1–2 branches to the stomach. LN dissection of station 6 (infrapyloric area) was performed with a preservation of the infrapyloric artery and vein as the same method used in the pylorus-preserving gastrectomy, and the right gastroepiploic artery was ligated after the branching of the infrapyloric artery [11].

LN station 3a and about proximal half of 3b was dissected in all four acute experiments with a ligation of right gastric artery after branching of 3–4 vessels to the stomach. In the survival model, two pigs (survival group A) underwent the same extent of LN dissection of the lesser curvature (3a + half of 3b), and the other two pigs (survival group B) underwent full 3a and 3b dissection with a ligation of the right gastric artery just after the first 1–2 branch near the pylorus.

Multiple horizontal mattress sutures were placed using an endoscopy–laparoscopy hybrid method as described before [12] (Figs. 1C, D, 3). A laparoscopic suture-passer prototype carrying 2-0 nylon suture was introduced into the abdominal cavity and bended. The gastric wall just outside of the marked resection line around the pseudo-tumor was penetrated by the suture-passer, and the thread was delivered to the endoscopic alligator grasper. The other side of the resection line was penetrated by an empty suture-passer, and received a suture from the endoscopic grasper. This maneuver is repeated in reverse direction to make a horizontal mattress suture around the tumor, and the suture was fastened and tied. Additional multiple horizontal mattress sutures were progressively placed until the whole marked resection line was covered by the sutures. Selectively, a straight needle with 2-0 nylon suture was used to make horizontal mattress sutures when it is favorable due to an approximation of the proximal and distal resection line caused by previous sutures.

After completion of multiple sutures, laparoscopic linear staplers were applied beneath the sutures to resect the pseudo-tumor and the possible lymphatic spreading pathway shown by fluorescent signal. The specimen was removed through one of the trocar sites, after enlarging the incision. The length of the specimen, at lesser curvature side and greater curvature side, and the surface area were

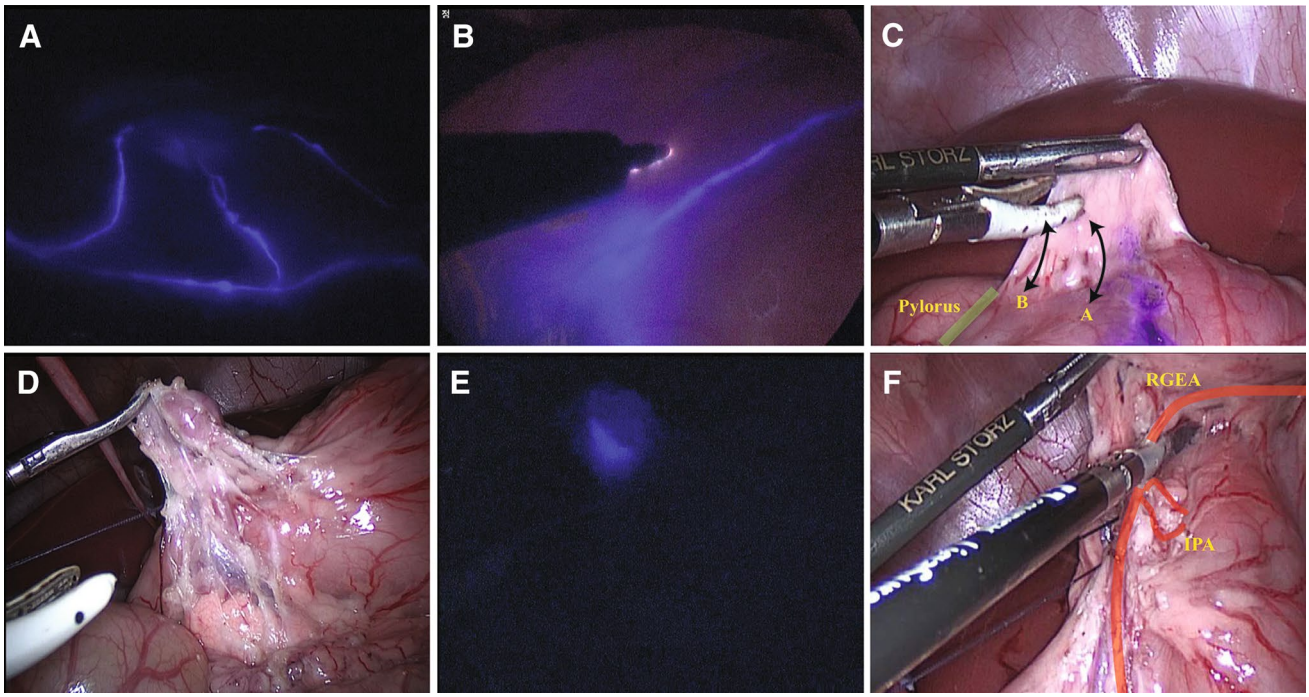


**Fig. 2** Extent of the resection. **A** Possible lymphatic spreading pathway in the gastric wall highlighted by fluorescent signal; **B** resection line was marked by an electro-cautery; **c** extent of the lymph node dissection in lesser curvature side. Line A preserves 3–4 branches of the gastric artery for acute models and group A in survival models. Line B preserves 1–2 branches for group B; **D**–**F** Lymph node dissection of infrapyloric area. The right gastroepiploic artery was ligated after a branching of the infrapyloric artery

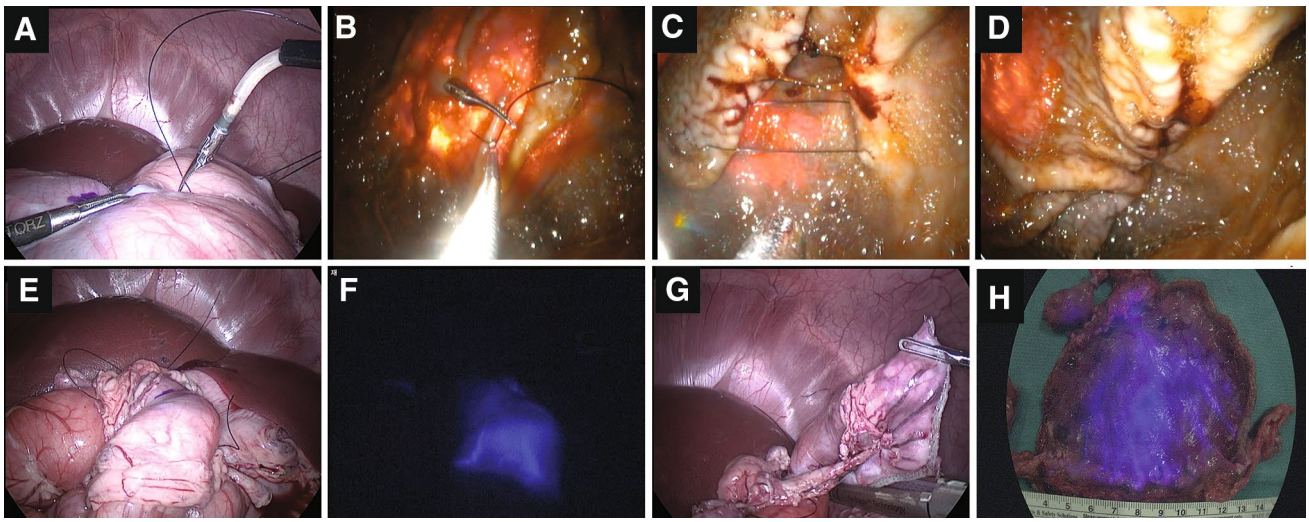


**Fig. 3** Hybrid endoscopy/laparoscopy non-exposed resection technique. **A**–**C** Cooperative procedure between a laparoscopic suture-passer and endoscopic grasper made multiple horizontal mattress sutures. **D**–**F** After sutures, fastening of the sutures forms a mushroom-like structure containing the primary tumor and the lymphatic pathways; **G** linear staplers were applied beneath the sutures to resect the whole specimen; **H** the specimen resected with enough resection margin. It shows more diffused fluorescent signal compared with those at the beginning of the operation

measured using an open source software (imageJ®, available at: http://www.imagej.net).

### Evaluation of the perfusion of the remaining posterior wall

ICG (0.5 mg/kg in concentration of 2.5 mg/ml) was intravenously injected to visually evaluate the perfusion to the remnant stomach, especially the posterior wall of the resection site which has a high probability of ischemia due to devascularization of both lesser and greater curvature (Fig. 4). Capillary lactate test was performed at four points on the posterior wall of the resection site (proximal/distal, lesser curvature/greater curvature side) as well as at a point near the short gastric artery (stomach control) and at the pig's snout (systemic control) to evaluate the tissue ischemia. Gastric wall was superficially cut by laparoscopic scissors, and blood was aspirated by means of a falcon tube attached to a motorized pipette, and the level was measured using a kit as previously described [13–18] (Figs. 1F, 4C). The ratio of capillary lactate level (stomach sampling site/systemic control) ≥ 3 and/or absolute value ≥ 3 mmol/l was preliminarily regarded as a cut-off value of possible ischemia, and was correlated with clinical manifestation.

### Gastric motility function

Food intake was daily calculated after operation with a measurement of the amount of provided food and remaining food after eating. The amount of food residue in the remnant stomach was observed by endoscopy at the beginning of the procedure 7 days after surgery in survival models.

A dynamic MRI was performed to evaluate gastric peristalsis in two cases of acute models and in all of the survival models using 1.5 T system (Magnetom Aera®, Siemens; Munich, Germany). Baseline test was performed before the procedure, and repeated right after procedure in acute models and 7 days later in survival models. Gastric content was aspirated by endoscopy, and a nasogastric tube was inserted through the mouth into the stomach. Five hundred milliliters of pineapple juice were injected into the stomach via the nasogastric tube. Different positions (supine, prone, and right decubitus) of pig were tried in an exploratory purpose. The parameter of the dynamic sequence (TrueFISP) consists of a field of view 30 * 30 $cm^2$, 1 5-mm thick slice, TE/TR = 1.27 ms/759 ms, flip angle 54°, fat saturation, in plane resolution 192 × 192 pixels yielding 1.56 × 1.56 $mm^2$ pixels. The acquisition time was 1 min 1 s for 80 images with apnea, and the acquisitions were repeated 10 times with 3–5 min of recovery time between each acquisition.

The intensity of peristalsis was categorized as "strong" (amplitude of the contraction > 30% of the lumen) and "weak" (amplitude of the contraction < 30% of the lumen), and the frequency of the peristalsis was counted in recorded images reconstructed as movie clips.

## Results

### Technical feasibility of the fluorescent-guidance hybrid single-wall segmental resection with bilateral lymph node basin dissection (see Video 1 in Electronic Supplementary Material)

Fluorescent signals in the lymphatic channel in the gastric wall were clearly identified right after the endoscopic injection of ICG in both lesser curvature side and greater curvature side in all cases (Fig. 2A, B).

In all acute but case 4, infrapyloric LN was highlighted as a sentinel lymph node (Table 1). In case 3 in acute model and case B2 in survival model, lymph nodes located in posterior side of lesser curvature (LN station 3) were highlighted.

LN dissection of station 4d, 6, 3a, and 3b (only in survival group B) were performed.

Five or six horizontal mattress sutures were successfully placed by means of hybrid endoscopy–laparoscopic method

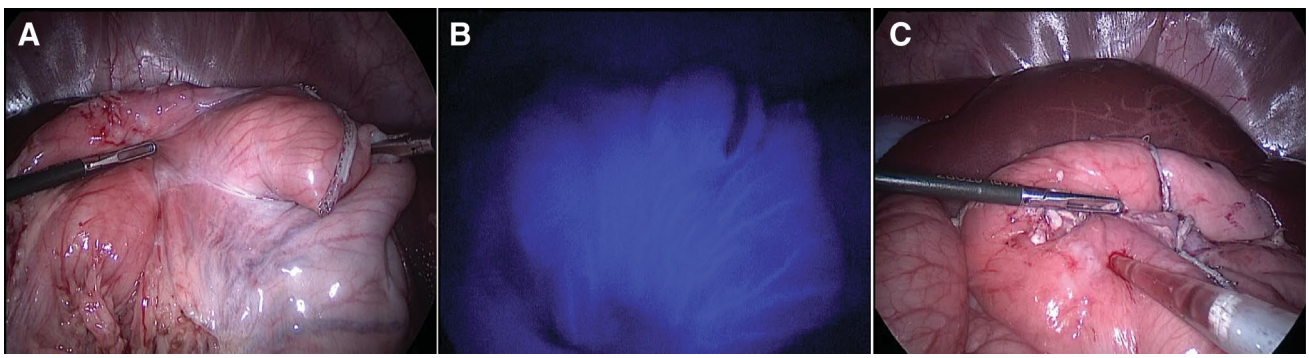


**Fig. 4** Evaluation of remaining stomach perfusion. Tests to evaluate the perfusion in the remaining posterior wall by **A** visual observation under a white light, **B** fluorescent angiography after intravenous injection of ICG, and **C** capillary blood sampling and test of lactate level

**Table 1** Operative procedure data

| No. | Body weight | Operative time (min) | Specimen size | | | Sentinel node station |
|---|---|---|---|---|---|---|
| | | | LC (cm) | GC (cm) | Surface area ($cm^2$) | |
| Acute models | | | | | | |
| 1 | 30.0 | 67 | 4 | 6.5 | 38.6 | # 6 |
| 2 | 32.0 | 110 | 4.8 | 12.8 | 83.9 | # 6 |
| 3 | 33.5 | 106 | 4 | 12 | 81.4 | # 6 |
| 4 | 34.1 | 92 | 4.4 | 10.8 | 64.8 | # 3 |
| Survival group A | | | | | | |
| A1 | 32.3 | 76 | 5.1 | 8.2 | 46.7 | # 6 |
| A2 | 34.9 | 91 | 4.2 | 10.8 | 71.3 | # 6 |
| Survival group B | | | | | | |
| B1 | 33.3 | 91 | 3.8 | 8.3 | 45.9 | # 6 |
| B2 | 30.0 | 115 | 5.5 | 10.5 | 68.7 | # 3 and # 6 |
| Mean ± SD | 32.5 ± 1.8 | 93.5 ± 16.5 | 4.5 ± 0.6 | 10.0 ± 2.1 | 62.7 ± 17.0 | |

*LC* lesser curvature, *GC* greater curvature, *SD* standard deviation, *station #3* lesser curvature lymph nodes, *station #6* infrapyloric lymph nodes

without significant spillage or bleeding. After fastening the sutures, the gastric wall was out pouched in a "mushroom" shape and included the area of a pseudo-tumor and all the area in the gastric wall showing fluorescent signal (Fig. 3F, H).

Linear staplers could be applied perpendicularly to the long axis of the stomach, and the whole mushroom and dissected lymph nodes could be removed together.

Mean operation time (excluding time for trocar placement and skin wound repair) was 93.5 ± 16.5 min (min 67, max 15). The length of the lesser and greater curvature side and the surface area of the specimen were 4.5 ± 0.6 cm (min 4.0, max 5.5), 10.0 ± 2.1 cm (min 6.5, max 12.8), and 62.7 ± 17.0 $cm^2$ (min 38.6, max 83.9), respectively.

Endoscopic observation after the resection found no evidence of leakage or stenosis at the anastomosis site.

### Ischemia of the remaining stomach

Immediately after injection of ICG intravenously, the gastric wall of the remaining stomach was uniformly highlighted by the fluorescent signal. The perfusion represented by fluorescent signal in the posterior wall was as bright and diffuse as in other part of the stomach (Fig. 3H).

Possibly ischemic area presumed with criteria of the lactate level ratio (stomach/systemic) ≥ 3 and the absolute value ≥ 3 mmol/l is found only one case; survival model B2 at the greater curvature side, distal area. However, this site was well-perfused in the fluorescent imaging after systemic ICG injection, and return to a level below the criteria 7 days later. Points with lactate level ratio ≥ 3 were higher in survival group B2 compared to other groups; 2 out of 4 spots in B1and 3 out of 4 spots in B2. All these points were also well-perfused in the fluorescent imaging (Fig. 5) (Table 2).

### Function (see Video 2 in Electronic Supplementary Material)

There was no significant impairment of overall general condition or activity in all the 4 survival pigs. Pigs with limited lesser curvature dissection (A1 and A2) ate all the provided food, and there was almost no remnant food in the follow-up endoscopy on POD7. On the other hand, B1 in the group of complete LN 3 station ate all the provided food but presented with vomiting on POD7, and B2 pig could intake only 1/3 of the provided food. Follow-up endoscopic finding showed large amount of remnant food in B1 and B2 pigs (Table 3).

The mean frequency of peristalsis counted by a dynamic MRI was 2.5 ± 0.6 times/min in pre-operative period in all six pigs. The frequency remained constant in the acute pigs, immediately after the operation, as well as in A1 and A2 pigs in the survival model on POD7. Conversely, the peristalsis could hardly be identified in B1 and B2 pigs on POD7, and the frequency was significantly lower than pre-operative controls.

## Discussion

Lymphatic metastasis is the most frequent mode of metastasis in gastric cancer and a complete dissection of the metastatic lymphatic tissues can significantly increase the survival rate [19, 20].

The standard radical surgery for gastric cancer is composed of resection of large proportion of the stomach (2/3 of the stomach) and wide lymph node dissection. Such a wide dissection is needed to completely remove all the lymphatic channels in the gastric wall and extra-gastric

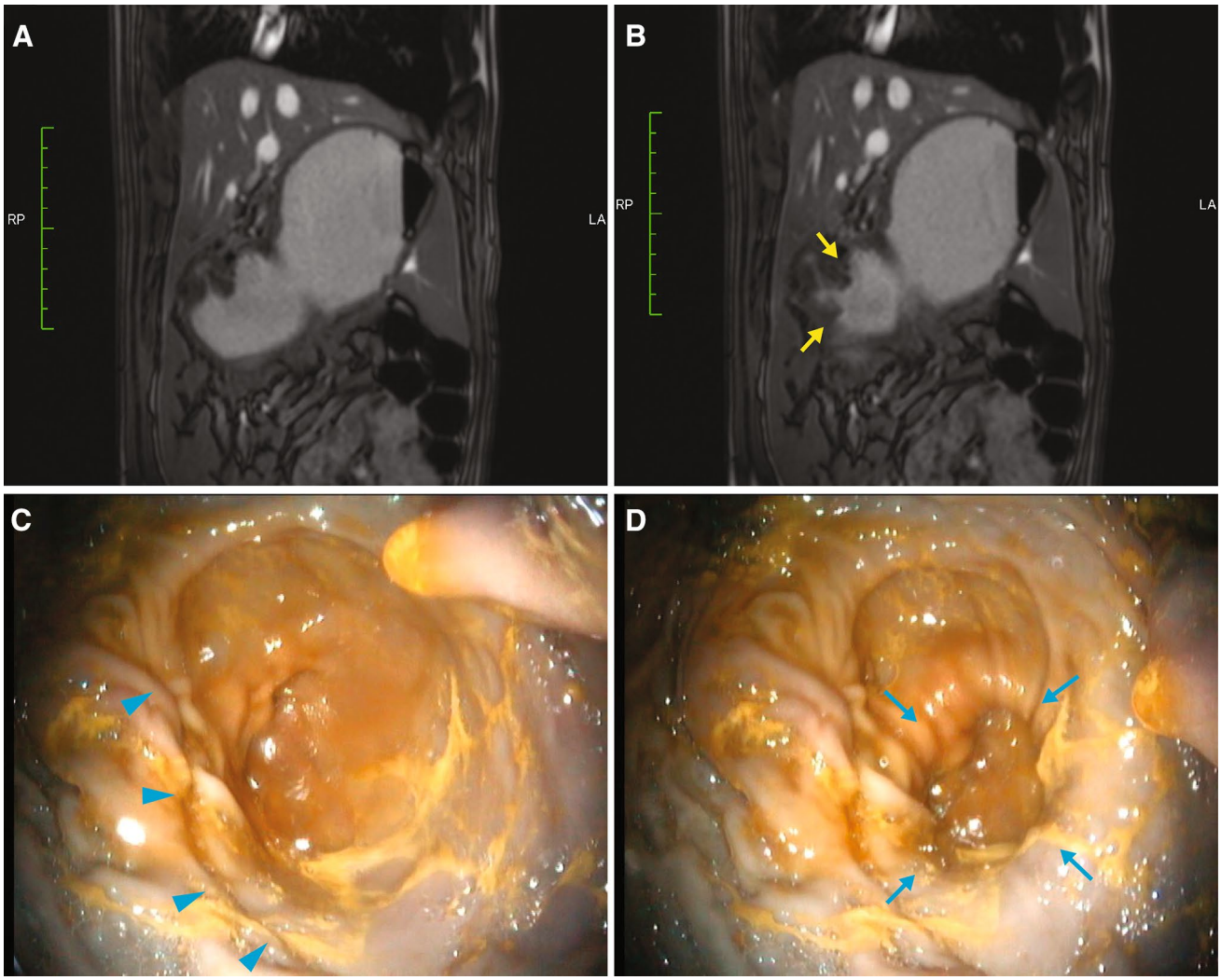


**Fig. 5** Gastric motility evaluation. Symmetric contractions (arrows) are maintained in the remaining antrum 7 days after operation in group A survival pigs. **A, B** A dynamic MRI images; **C, D** endoscopic view. Arrowheads indicate a stapling line

lymphatic tissues, because the cancer spreading pathway of the individual gastric cancer cannot be accurately anticipated [21].

Sentinel lymph node navigation (SLN) surgery has been investigated for gastric cancer to limit and tailor the extent of the lymph node dissection. Reduced extent of lymph node dissection may reduce some local surgical complications such as intra-abdominal abscess. However, the post-operative quality of life after gastrectomy may not be greatly improved by the limited lymphadenectomy since post-gastrectomy syndromes, including dumping, diarrhea, or delayed gastric emptying and the amount of oral intake are more related to the extent of the gastric resection itself. In fact, a reduced gastric resection, such in that achieved with a pylorus-preserving gastrectomy, is associated with less occurrence of post-gastrectomy syndrome and better preservation of nutritional profile [22].

The lymphatic spreading pathway inside the gastric wall is invisible and not predictable, which is one of the reasons for designing a radical gastrectomy as resecting 2/3 of the stomach. Near-infrared fluorescent imaging using submucosal injection of ICG is a promising method of SLN, because of its high sensitivity, relatively high tissue depth penetration, and no biohazard [9, 23]. SLN enables also the visualization of the lymphatic channels within the gastric wall. The lymphatic channels highlighted by fluorescence imaging signals, can serve as possible indicators of the extent of a local FTR, which could eliminate all the viable cancer cells which could remain in the lymphatic tissues within the gastric wall even when the sentinel lymph node is metastasis free.

We have used a quite low concentration (0.1 mg/ml) and small volume (1 ml) of ICG to visualize the gastric lymphatic channels. A large amount of ICG can diffuse too

**Table 2** Capillary lactate level at the posterior wall of the resection site after operative procedure

| No. | Immediately after resection | | | | | | 7 days after resection | | | | | |
|---|---|---|---|---|---|---|---|---|---|---|---|---|
| | Snout | Fundus | GC, dist. | LC, dist. | GC, prox. | LC, prox. | Philtrum | Fundus | GC, dist. | LC, dist. | GC, prox. | LC, prox. |
| Acute model | | | | | | | | | | | | |
| 1 | NA | NA | NA | NA | NA | NA | | | | | | |
| 2 | 0.8 | 0.5 (0.6) | 2.3 (2.9) | 1.1 (1.4) | 0.5 (0.6) | 1.5 (1.9) | | | | | | |
| 3 | 0.5 | 1.8 (3.6) | 0.5 (1.0) | 0.5 (1.0) | 0.5 (1.0) | 0.5 (1.0) | | | | | | |
| 4 | 2.4 | 3.1 (1.3) | 1.8 (0.8) | 2.4 (1.0) | 3.0 (1.3) | 2.2 (0.9) | | | | | | |
| Survival group A | | | | | | | | | | | | |
| A1 | 2.2 | NA | 4.4 (2.0) | 1.6 (0.7) | 2.4 (1.1) | 2.0 (0.9) | 3.2 | 3.4 (1.1) | 5.1 (1.6) | 2.1 (0.7) | 5.0 (1.6) | 6.2 (1.9) |
| A2 | 1.0 | 1.0 (1.0) | 1.8 (1.8) | 1.0 (1.0) | 1.0 (1.0) | 0.5 (0.5) | 0.9 | 1.2 (1.4) | 1.5 (1.7) | 1.1 (1.3) | 1.0 (1.2) | 0.9 (1.1) |
| Survival group B | | | | | | | | | | | | |
| B1 | 0.5 | 0.5 (1.0) | 1.7 (3.4) | 2.0 (4.0) | 0.8 (1.6) | 0.5 (1.0) | 0.8 | 1.5 (1.9) | 1.1 (1.4) | 1.2 (1.5) | 2.6 (3.3) | 0.6 (0.8) |
| B2 | 0.5 | 1.2 (2.4) | **5.0 (10.0)** | 1.5 (3.0) | 1.2 (2.4) | 2.1 (4.2) | 2.1 | 3.4 (1.6) | 3.1 (1.5) | 2.0 (1.0) | 2.7 (1.3) | 3.7 (1.8) |

Values are presented as mmol/L, and the values in the parenthesis are the ratio of the level over the that of the systemic control (pig's snout). Fundus is a control in the stomach. The values of which the absolute level > 3.0 and the ratio > 3.0 was represented as bold characters

*LC* lesser curvature, *GC* greater curvature, *dist*. distal area, *prox*. proximal area

widely at the injection site and cover a large proportion of the gastric wall, and thus might prevent from a meaningful tailored surgery [9]. To prevent from accidental extra-gastric spillage of ICG, we used a double injection technique, similar to that used for tattooing of colon cancer. In fact, the body of the porcine gastric wall is sometimes hard to inject submucosally, and a spillage of ICG outside of the lumen of the stomach, could have significantly impaired the fluorescent view with a highly bright staining. Therefore, we injected 0.5 ml of saline first to make a bleb, and then injected 0.5 ml of 0.2 mg/ml of ICG inside of the bleb [24]. Although it is easier to perform a submucosal injection in the human stomach, this technique could be used during the learning curve to avoid extra-gastric leakages. The lymphatic channels within the gastric wall could be clearly identified by the near-infrared camera system right after injection. We observed that the fluorescent signal became blurred and diffused a couple of hours after the injection, due to the low molecular weight and the rapidly diffusing characteristics of the ICG. Therefore, we suggest to perform the determination of the resection line right after the injection.

One of the challenges in FTR for gastric cancer is to prevent free cancer cells spillage into the peritoneal cavity. In a previous study, we observed the presence of free cancer cells in the gastric lumen, even in case of early gastric cancer [25]. Hence, there is a theoretical possibility of peritoneal seeding through a widely opened gastric wall during FTR. A few "non-exposed" endoscopy/laparoscopy cooperative full-thickness resection techniques, such as "NEWS" or "CLEAN-NET", have been suggested, to reduce this risk [4, 26, 27]. Those techniques are ingenious and feasible, however, there are some drawbacks such as the need of long-time involvement of highly skilled endoscopists, long operation time, or limitation of the specimen size (< 3 cm) which is not feasible to be applied to the new concept of resection to remove the primary tumor as well as the lymphatic channels connected to the sentinel lymph nodes. We have designed a new non-exposed hybrid FTR technique using a laparoscopic trans-gastric suture passer, which makes sutures around the tumor to generate a mushroom-like specimen and enable an easy stapling in a desirable direction [12]. In the present experiment, we have used a similar technique, except that we preferred multiple interrupted horizontal mattress over a continuous suturing. The other difference was that, in the present study, the size of the specimen was much larger.

Mean operation time to remove a large specimen (lesser curvature side: 4.0–5.5 cm, grater curvature side: 6.5–12.8 cm) and to perform a bilateral lymph node dissection with a preservation of the infrapyloric artery was 1 h 30 min. Compared to the operation time of other types of non-exposed as long as 2–5 h for the specimen < 3–5cm, it can be regarded as a relatively fast procedure [4]. As discussed in a previous report, the advantages of this technique include a fast operation time, an easier endoscopic performance, which can be dealt with moderately experienced endoscopy, an easy control of the stapling line, and the applicability to large non-round specimen. All those advantages were confirmed in the present study.

We designed one of extreme scenarios for a local FTR to examine a general feasibility of the procedure: a tumor located in the anterior wall of which the lymphatic spreading pathways are both to the lesser and the greater curvature side. In our previous analysis on gastric cancer with 1–3 metastatic lymph nodes, tumors located at anterior or posterior wall of the body or the antrum of the stomach had a lymph node metastasis at the lesser curvature side in about

**Table 3** Gastric function after operation evaluated by measurement of food intake, residual food in endoscopy, and frequency of gastric peristalsis in a dynamic MRI

| No. | Body weight change (kg) | Food intake (g/d) | Adverse events | Residual food in endoscopy | Frequency of gastric peristalsis measured by dynamic MRI | | | | | |
|---|---|---|---|---|---|---|---|---|---|---|
| | | | | | Pre-operative (times/min) | | | Post-operative (times/min) | | |
| | | | | | Strong | Weak | Total | Strong | Weak | Total |
| Acute experiment | | | | | | | | Immediately after resection | | |
| 2 | | NA | NA | NA | 2.5 | 0.2 | 2.7 | 1.7 | 0.4 | 2.1 |
| 4 | | NA | NA | NA | 3.5 | 0.0 | 3.5 | 2.1 | 0.6 | 2.7 |
| Survival group A | | | | | | | | 7 day after resection | | |
| A1 | −0.3 | 875 | No | – | 0.0 | 2.2 | 2.2 | 2.8 | 0.2 | 3.0 |
| A2 | −2.7 | 858 | Loose stool (POD 1–3) | – | 1.6 | 0.6 | 2.2 | 0.1 | 1.8 | 1.9 |
| Survival group B | | | | | | | | | | |
| B1 | +2.0 | 875 | Vomiting (POD 7) | ++ | 1.5 | 1.0 | 2.5 | 0 | 0.4 | 0.4 |
| B2 | +3.5 | 295 | No | ++ | 0.0 | 1.7 | 1.7 | 0 | 0.2 | 0.2 |

50% and at the greater curvature side in also about 50%. The incidence of "transversal metastasis", which indicates the lymph node metastasis from the tumor located at either lesser or greater curvature side to the opposite curvature of the stomach in a "transverse" manner, was reported to occur in 16.7–41.2% and 4.3–50.8% for tumors located at lesser and greater curvature of the stomach, respectively [28–30].

The "single-wall segmental resection" was designed for this situation, in order to remove both the primary cancer site and the possible lymphatic spreading pathway guided by the ICG fluorescent signal and to preserve the other part of the stomach for a function-preservation. To estimate the benefits of the preservation of the remaining stomach, the resection technique was simulated in ex-vivo porcine stomachs. single-wall resections of the anterior and posterior wall as well as conventional segmental resection to resect both wall were simulated sequentially (Fig. 6). From simulations of resection of the part of the stomach (3 cm in the lesser curvature side and 7 cm in the greater curvature side), we could estimate that the single-wall resection will preserve about 10–20% more luminal volume when compared to segmental resection of the both gastric wall.

In spite of possible benefits of volume preservation, there were a few concerns about the procedure. It has been suggested that the lymph node basin dissection is safer than lymph node picking in the SLN in gastric cancer, because the metastatic non-sentinel nodes are usually found in the same basin of the examined sentinel nodes when the sentinel node is turned out to be negative and abandon further lymph node dissection [3]. Therefore, substantial extent of perigastric lymph node dissection may be needed for this tumors with a chance of bilateral (lesser and greater curvature) lymph node metastasis, to remove lymph node basins in both lesser and greater curvature side. In spite of well-developed vascular network of the gastric wall, this bilateral lymph node dissection may cause ischemia and denervation in remaining gastric wall theoretically.

We also paid attention to the wide resection of the anterior wall, because we experienced that a relatively large posterior wall remained after operation acts as a denervated non-functioning sac and caused delayed emptying after distal gastrectomy. Unlike distal gastrectomy, we hypothesized that the remaining antrum and the pylorus may play a role for gastric emptying, like in case of the pylorus-preserving gastrectomy. Therefore, the lymph node dissection was performed according to the pylorus-preserving gastrectomy technique, including the preservation of the infrapyloric artery and the pyloric branch of the hepatic branch of the anterior vagus nerve [11]. Considering the very short length of the lesser curvature of the porcine stomach, we preserved 3–4 branches to the antrum from the gastric artery in the acute model, and identified emptying movement in MRI. In the survival model, we repeated the same extent

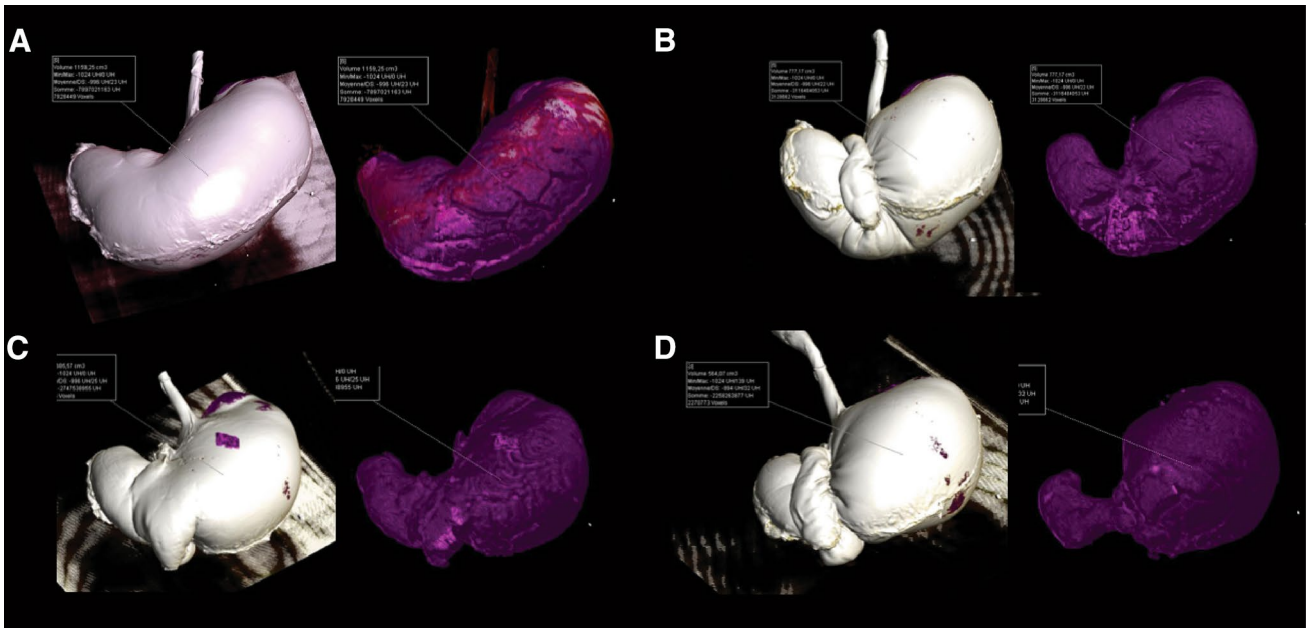


**Fig. 6** Simulation of the gastric resection. Simulation of the resection of anterior wall, posterior wall, and both walls to remove the gastric wall with a boundary of 3 cm of the lesser curvature and 7 cm of the greater curvature. Calculated volume with a fixed intragastric pressure (10 mmHg) was **A** 1159 $cm^3$ before resection, **B** 777 $cm^3$ after anterior wall resection, **C** 686 $cm^3$ after posterior wall resection, and **D** 564 $cm^3$ after resection of both walls

of resection in two pigs (A1 and A2) and also we tested a larger dissection of the lymph node station 3b preserving only 1–2 branches as per the pylorus-preserving gastrectomy in human (B1 and B2).

In this setting, several explorative methods were chosen to examine the blood perfusion and the function of the remaining stomach. In spite of the wide devascularization of both lesser and greater curvature side, the color of the remaining posterior wall of the stomach remained pinkish in observation by white light images. We also performed a fluorescence-based angiography by systemic ICG injection to qualitatively evaluate the perfusion. This method is currently actively been investigated to estimate the perfusion in colorectal or esophagogastric anastomosis [31, 32].

The whole gastric wall was evenly and rapidly highlighted with the fluorescent signal of ICG, regardless of the extent of the dissection at the lesser curvature side. Despite in this setting we did not use a computer-assisted quantitative measure of the fluorescence signal [33], the rapidity of the tissue enhancement by the fluorophore is a good marker of the presence of blood supply.

The local capillary lactate test was found to be a very sensitive indicator of ischemia in our previous experiments for the small bowel and the colon. A cut-off value predictive of improved anastomotic healing seemed to be $> 2$ of capillary lactates local to systemic ratio [13, 14, 33]. However, the stomach had higher basal capillary lactates local to systemic ratio when compared to bowel, as high as 1.5–2.0, possibly due to more complex vascular network and different metabolic activity [15]. From the previous data, we arbitrarily set the presumed cut-off value as capillary lactates local to systemic ratio $\geq 3$ and actual capillary lactates level $\geq 3$ mmol/L. There was a tendency that the survival group B had more points of lactates ratio $\geq 3$ compared with acute model or survival group A. Although almost all points return to normal range 7 days after surgery, there is a chance that the larger devascularization of the lesser curvature side could play a role together with denervation to result in functioning loss in group B pigs. Further researches about the normal and pathologic cut-off value of the capillary lactate are needed.

The function of the stomach was dramatically different between survival group A and B depending on the extent of the lymph node dissection in the lesser curvature side. Pigs in group A took all the provided food with no residual food in the stomach, however, pigs in group B could not eat provided food well or vomited with a large amount of residual food in the remaining stomach. We interpret these result as that the denervation of the antrum from the pyloric branch of the vagus nerve that caused a loss of peristalsis function of the antrum in group B.

A dynamic MRI was also used to evaluate the function and movements of the stomach. This exam has already been tested in humans, and is expected to provide a more real time information about the cause of a functional

deterioration when compared to a gastric emptying scintigraphy using radioisotopes [34–36].

There have been no investigations about bowel function using a dynamic MRI in the pig, probably because it cannot be done in awaking animals and because there have been rare needs to test the functional outcome of a new surgical procedure in the stomach. We expect that this technology can be useful to evaluate the function of the stomach after a new surgical procedure in preclinical validation steps. We used propofol-based totally intravenous anesthesia without muscle relaxants to minimize the effect of the drug to the bowel function. Pineapple juice, which has been reported as a good intraluminal contrast for MRI, was instilled inside of the stomach [37, 38]. The dynamic MRI provided good visual information on the peristaltic movements and on how the mixing of the food occurs. Gastric movements can be affected by multiple factors, including the status of fasting or the stress during the premedication process before the main anesthesia. The gastric movement is known to be composed of tonic contractions of the stomach ('pressure pump') or antral contraction waves (ACW) ('peristaltic pump'), which are independent but coordinated with each other [39]. We categorized the observed movements as "strong" and "weak" based on the amplitude of the peristalsis, and weak peristalsis may accompany tonic contraction of the stomach. We could not calculate the exact contraction movement but categorized them more qualitatively, because only one plane can be selected for the acquisition of the dynamic MRI, and the plane could not cover the exact center of the pylorus and the whole stomach, especially in the post-operative period. The contraction may be calculated accurately if the plane is passing through the center of the lumen, but it could be exaggerated if the plane is far from the center. If a multi-axis acquisition dynamic MRI could be developed, it could be more useful for a complete understanding of the whole stomach and the accurate quantitative measurement of the strength of the peristalsis, especially in the stomach deformed by surgery.

There are some limitations in this study. First, the study was composed of small sample size. Secondly, there are some anatomic differences between the porcine and human stomach. Particularly, the end branches of the nerve of Latarjet, which runs through the whole lesser curvature, is supposed to be preserved in the highly selective vagotomy to preserve the emptying function of the antrum in human. The human stomach can function after the pylorus-preserving gastrectomy with this nerve cut. However, it should be revalidated in humans whether the emptying function could be preserved after a wide local FTR as we have performed in this study. Thirdly, applicability of cases with distal sentinel lymph nodes located in the D2 area could not be evaluated due to the limited number of cases and some anatomical differences between humans and pigs. Finally, a normal meal was provided, instead of a soft meal adapted for post-gastrectomy feeding. We expected that the normal meal could be tolerable after the local resection at the beginning. However, it could have been difficult to digest with a partially denervated stomach.

In summary, we have provided the proof of concept of a local FTR strategy guided by fluorescent intragastric lymphangiography accompanied by a bilateral sentinel lymph node basin dissection using a diluted concentration of ICG. This fluorescent intra-parietal-gastric lymphangiography, per se, is expected to provide information and guidance for the extent of the gastric resection, regardless of the detailed resection method. We have also validated the feasibility of a new non-exposed endoscopy/laparoscopy hybrid resection techniques in a relatively large non-round specimen and single-wall gastric resection with bilateral lymph node basin dissection, identifying the preserved emptying function of the stomach in case of the limited dissection of the lesser curvature side. The possibility of a loss of emptying function after radical dissection of the lesser curvature of the stomach was noted, and safe extent of lymph node dissection should be cautiously determined in further human studies.

**Acknowledgements** This study was supported by an IHU-Strasbourg feasibility Grant (PI: Pr. Seong-Ho Kong) and by the ELIOS (Endoscopic Luminescent Imaging for precision Oncologic Surgery) project grant. Michele Diana is the recipient of the ELIOS project grant from the ARC foundation for Cancer Research, aiming at the development of fluorescence-guided surgery.

## Compliance with ethical standards

**Disclosures** Jacques Marescaux is the President of both IRCAD and IHU-Strasbourg Institutes, which are partly funded by Karl Storz, Medtronic and Siemens. Authors Seong-Ho Kong, Francesco Marchegiani, Renato Soares, Yu-Yin Liu, Yun-Suhk Suh, Hyuk-Joon Lee, Dallemagne B, Han-Kwang Yang and Michele Diana have no conflicts of interest or financial ties to disclose.

## References

1. Maruyama K, Sasako M, Kinoshita T, Sano T, Katai H (1999) Can sentinel node biopsy indicate rational extent of lymphadenectomy in gastric cancer surgery? Fundamental and new information on lymph-node dissection. Langenbeck's Arch Surg 384:149–157
2. Ahn HS, Lee HJ, Hahn S, Kim WH, Lee KU, Sano T, Edge SB, Yang HK (2010) Evaluation of the seventh American Joint Committee on Cancer/International Union Against Cancer Classification of gastric adenocarcinoma in comparison with the sixth classification. Cancer 116:5592–5598
3. Kitagawa Y, Takeuchi H, Takagi Y, Natsugoe S, Terashima M, Murakami N, Fujimura T, Tsujimoto H, Hayashi H, Yoshimizu N, Takagane A, Mohri Y, Nabeshima K, Uenosono Y, Kinami S, Sakamoto J, Morita S, Aikou T, Miwa K, Kitajima M (2013) Sentinel node mapping for gastric cancer: a prospective multicenter trial in Japan. J Clin Oncol 31:3704–3710

4. Hiki N, Nunobe S, Matsuda T, Hirasawa T, Yamamoto Y, Yamaguchi T (2015) Laparoscopic endoscopic cooperative surgery. Dig Endosc 27:197–204
5. Gotoda T, Yanagisawa A, Sasako M, Ono H, Nakanishi Y, Shimoda T, Kato Y (2000) Incidence of lymph node metastasis from early gastric cancer: estimation with a large number of cases at two large centers. Gastric Cancer 3:219–225
6. Oh SY, Lee KG, Suh YS, Kim MA, Kong SH, Lee HJ, Kim WH, Yang HK (2017) Lymph node metastasis in mucosal gastric cancer: reappraisal of expanded indication of endoscopic submucosal dissection. Ann Surg 265:137–142
7. Fujimura T, Fushida S, Tsukada T, Kinoshita J, Oyama K, Miyashita T, Takamura H, Kinami S, Ohta T (2015) A new stage of sentinel node navigation surgery in early gastric cancer. Gastric Cancer 18:210–217
8. Goto O, Takeuchi H, Sasaki M, Kawakubo H, Akimoto T, Fujimoto A, Ochiai Y, Maehata T, Nishizawa T, Kitagawa Y, Yahagi N (2016) Laparoscopy-assisted endoscopic full-thickness resection of gastric subepithelial tumors using a nonexposure technique. Endoscopy 48:1010–1015
9. Kong SH, Noh YW, Suh YS, Park HS, Lee HJ, Kang KW, Kim HC, Lim YT, Yang HK (2015) Evaluation of the novel near-infrared fluorescence tracers pullulan polymer nanogel and indocyanine green/gamma-glutamic acid complex for sentinel lymph node navigation surgery in large animal models. Gastric Cancer 18:55–64
10. Lee JH, Lee MS, Kim HH, Park DJ, Lee KH, Hwang JY, Lee HJ, Yang HK, Lee KU (2011) Feasibility of laparoscopic partial gastrectomy with sentinel node basin dissection in a porcine model. Surg Endosc 25:1070–1075
11. Nunobe S, Hiki N, Fukunaga T, Tokunaga M, Ohyama S, Seto Y, Yamaguchi T (2007) Laparoscopy-assisted pylorus-preserving gastrectomy: preservation of vagus nerve and infrapyloric blood flow induces less stasis. World J Surg 31:2335–2340
12. Kong SH, Diana M, Liu YY, Lee HJ, Legner A, Soares R, Swanstrom L, Dallemagne B, Yang HK, Marescaux J (2016) Novel method for hybrid endo-laparoscopic full-thickness gastric resection using laparoscopic transgastric suture passer device. Surg Endosc 30:1683–1691
13. Diana M, Noll E, Diemunsch P, Dallemagne B, Benahmed MA, Agnus V, Soler L, Barry B, Namer IJ, Demartines N, Charles AL, Geny B, Marescaux J (2014) Enhanced-reality video fluorescence: a real-time assessment of intestinal viability. Ann Surg 259:700–707
14. Diana M, Noll E, Diemunsch P, Moussallieh FM, Namer IJ, Charles AL, Lindner V, Agnus V, Geny B, Marescaux J (2015) Metabolism-guided bowel resection: potential role and accuracy of instant capillary lactates to identify the optimal resection site. Surg Innov 22:453–461
15. Diana M, Halvax P, Pop R, Schlagowski I, Bour G, Liu YY, Legner A, Diemunsch P, Geny B, Dallemagne B, Beaujeux R, Demartines N, Marescaux J (2015) Gastric supply manipulation to modulate ghrelin production and enhance vascularization to the cardia: proof of the concept in a porcine model. Surg Innov 22:5–14
16. Diana M, Dallemagne B, Chung H, Nagao Y, Halvax P, Agnus V, Soler L, Lindner V, Demartines N, Diemunsch P, Geny B, Swanstrom L, Marescaux J (2014) Probe-based confocal laser endomicroscopy and fluorescence-based enhanced reality for real-time assessment of intestinal microcirculation in a porcine model of sigmoid ischemia. Surg Endosc 28:3224–3233
17. Diana M, Halvax P, Dallemagne B, Nagao Y, Diemunsch P, Charles AL, Agnus V, Soler L, Demartines N, Lindner V, Geny B, Marescaux J (2014) Real-time navigation by fluorescence-based enhanced reality for precise estimation of future anastomotic site in digestive surgery. Surg Endosc 28:3108–3118
18. Diana M, Pop R, Beaujeux R, Dallemagne B, Halvax P, Schlagowski I, Liu YY, Diemunsch P, Geny B, Lindner V, Marescaux J (2015) Embolization of arterial gastric supply in obesity (EMBARGO): an endovascular approach in the management of morbid obesity. Proof of the concept in the porcine model. Obes Surg 25:550–558
19. Mocellin S, Nitti D (2015) Lymphadenectomy extent and survival of patients with gastric carcinoma: a systematic review and meta-analysis of time-to-event data from randomized trials. Cancer Treat Rev 41:448–454
20. Kong SH, Lee HJ, Ahn HS, Kim JW, Kim WH, Lee KU, Yang HK (2012) Stage migration effect on survival in gastric cancer surgery with extended lymphadenectomy: the reappraisal of positive lymph node ratio as a proper N-staging. Ann Surg 255:50–58
21. Association JGC (2017) Japanese gastric cancer treatment guidelines 2014 (ver. 4). Gastric Cancer 20:1–19
22. Suh YS, Han DS, Kong SH, Kwon S, Shin CI, Kim WH, Kim HH, Lee HJ, Yang HK (2014) Laparoscopy-assisted pylorus-preserving gastrectomy is better than laparoscopy-assisted distal gastrectomy for middle-third early gastric cancer. Ann Surg 259:485–493
23. Yoshida M, Kubota K, Kuroda J, Ohta K, Nakamura T, Saito J, Kobayashi M, Sato T, Beck Y, Kitagawa Y, Kitajima M (2012) Indocyanine green injection for detecting sentinel nodes using color fluorescence camera in the laparoscopy-assisted gastrectomy. J Gastroenterol Hepatol 27(Suppl 3):29–33
24. Park JW, Sohn DK, Hong CW, Han KS, Choi DH, Chang HJ, Lim SB, Choi HS, Jeong SY (2008) The usefulness of preoperative colonoscopic tattooing using a saline test injection method with prepackaged sterile India ink for localization in laparoscopic colorectal surgery. Surg Endosc 22:501–505
25. Han TS, Kong SH, Lee HJ, Ahn HS, Hur K, Yu J, Kim WH, Yang HK (2011) Dissemination of free cancer cells from the gastric lumen and from perigastric lymphovascular pedicles during radical gastric cancer surgery. Ann Surg Oncol 18:2818–2825
26. Inoue H, Ikeda H, Hosoya T, Yoshida A, Onimaru M, Suzuki M, Kudo SE (2012) Endoscopic mucosal resection, endoscopic submucosal dissection, and beyond: full-layer resection for gastric cancer with nonexposure technique (CLEAN-NET). Surg Oncol Clin N Am 21:129–140
27. Goto O, Takeuchi H, Kawakubo H, Matsuda S, Kato F, Sasaki M, Fujimoto A, Ochiai Y, Horii J, Uraoka T, Kitagawa Y, Yahagi N (2015) Feasibility of non-exposed endoscopic wall-inversion surgery with sentinel node basin dissection as a new surgical method for early gastric cancer: a porcine survival study. Gastric Cancer 18:440–445
28. Lee JH, Lee HJ, Kong SH, Park do J, Lee HS, Kim WH, Kim HH, Yang HK (2014) Analysis of the lymphatic stream to predict sentinel nodes in gastric cancer patients. Ann Surg Oncol 21:1090–1098
29. Huang B, Wang Z, Sun Z, Zhao B, Xu H (2011) A novel insight of sentinel lymph node concept based on 1–3 positive nodes in patients with pT1-2 gastric cancer. BMC Cancer 11:18
30. Liu CG, Lu P, Lu Y, Jin F, Xu HM, Wang SB, Chen JQ (2007) Distribution of solitary lymph nodes in primary gastric cancer: a retrospective study and clinical implications. World J Gastroenterol 13:4776–4780
31. Sherwinter DA, Gallagher J, Donkar T (2013) Intra-operative transanal near infrared imaging of colorectal anastomotic perfusion: a feasibility study. Colorectal Dis 15:91–96
32. Degett TH, Andersen HS, Gogenur I (2016) Indocyanine green fluorescence angiography for intraoperative assessment of gastrointestinal anastomotic perfusion: a systematic review of clinical trials. Langenbeck's Arch Surg 401:767–775
33. Diana M, Agnus V, Halvax P, Liu YY, Dallemagne B, Schlagowski AI, Geny B, Diemunsch P, Lindner V, Marescaux J (2015) Intraoperative fluorescence-based enhanced reality laparoscopic

real-time imaging to assess bowel perfusion at the anastomotic site in an experimental model. Br J Surg 102:e169–e176
34. Baba S, Sasaki A, Nakajima J, Obuchi T, Koeda K, Wakabayashi G (2009) Assessment of gastric motor function by cine magnetic resonance imaging. J Gastroenterol Hepatol 24:1401–1406
35. Ajaj W, Lauenstein T, Papanikolaou N, Holtmann G, Goehde SC, Ruehm SG, Debatin JF (2004) Real-time high-resolution MRI for the assessment of gastric motility: pre- and postpharmacological stimuli. J Magn Reson Imaging 19:453–458
36. Curcic J, Sauter M, Schwizer W, Fried M, Boesiger P, Steingoetter A (2015) Validation of a golden angle radial sequence (GOLD) for abdominal T1 mapping during free breathing: demonstrating clinical feasibility for quantifying gastric secretion and emptying. J Magn Reson Imaging 41:157–164
37. Arthurs OJ, Graves MJ, Edwards AD, Joubert I, Set PA, Lomas DJ (2014) Interactive neonatal gastrointestinal magnetic resonance imaging using fruit juice as an oral contrast media. BMC Med Imaging 14:33
38. Zhang S, Olthoff A, Frahm J (2012) Real-time magnetic resonance imaging of normal swallowing. J Magn Reson Imaging 35:1372–1379
39. Kwiatek MA, Fox MR, Steingoetter A, Menne D, Pal A, Fruehauf H, Kaufman E, Forras-Kaufman Z, Brasseur JG, Goetze O, Hebbard GS, Boesiger P, Thumshirn M, Fried M, Schwizer W (2009) Effects of clonidine and sumatriptan on postprandial gastric volume response, antral contraction waves and emptying: an MRI study. Neurogastroenterol Motil 21:928–971